Assessment of Global TEC Mapping Using A Three-Dimensional Electron Density Model

Anthony J. Mannucci
Byron Iijima
Lawrence Sparks
Xiaoqing Pi
Brian Wilson
Ulf Lindqwister

Jet Propulsion Laboratory, California Institute of Technology
4800 Oak Grove Drive
Pasadena, CA 91109

Submission to special issue of Journal of Atmospheric and Solar-Terrestrial Physics, as proceedings to the following workshop held at JPL, December 1-3, 1998: *GPS Applications to the Structure and Dynamics of the Earth's Oceans and Ionosphere: Measurement, Analysis, Instrument Calibration, and Related Technologies.*

Contact information:
Corresponding author, A. J. Mannucci
Tel.: 001 818 354 1699; fax: 001 818 393 5115; e-mail: Tony.Mannucci@jpl.nasa.gov
All authors are at same address.

Abstract

Dual-frequency transmissions from the **Global Positioning System** satellites can be used to measure and map ionospheric **total electron content** (TEC) on global scales. Using data exclusively from ground-based **GPS** networks, global **ionosphere mapping** has been successfully applied using either two or three dimensional techniques. Two dimensional TEC maps retrieve a horizontally-varying distribution of total electron content, assuming a fixed vertical electron density profile. In **three dimensional mapping**, both the horizontal and vertical distribution of **electron density** are adjusted to fit the data. We describe a three-dimensional TEC mapping algorithm that uses three independent constant-density slabs stacked vertically to model the electron density, and compare with a more conventional two-dimensional approach using a single slab. One apparent benefit of the new method is reduction in a level error of the TEC maps, which decreased by 1.7 TECU using the three dimensional retrieval on simulated data (1 TEC Unit corresponds to 10^{16} electrons/m^2). Another benefit of the multilayer approach is improved slant TEC modeling. Using actual data from an equatorial site at Cocos Islands (96.8E, 12.2S), three

slab modeling improved estimates of slant TEC by a factor of 2 for elevation angles between 10 and 20 degrees (9 vs 4.4 TECU, root-mean-square). However, the global structure of the vertical TEC retrievals we analyzed did not improve using three dimensional modeling. This may due to a critical approximation shared by both techniques that TEC persists unchanged at a given local time. This assumption is required to produce global maps from observations acquired from widely scattered ground receivers. Further improving the retrieval of global TEC structure with ground-based data probably requires improved dynamical models of TEC behavior. New data available from GPS receivers in low Earth orbit is also promising.

1. Introduction

Continuously available transmissions from the constellation of twenty-four Global Positioning System (GPS) satellites are finding wide use for ionospheric research and applications. GPS signals allow line-of-sight total electron content (TEC) measurements between any GPS receiver and six to twelve satellites in view simultaneously. The National Aeronautics and Space Administration (NASA) uses GPS to calibrate signal propagation delays due to the Earth's ionosphere for a network of antennas tracking objects in space. With the advent of worldwide GPS ground receiver networks for geodetic research, we have developed a mapping technique that provides "snapshots" of the global TEC distribution updated every 15 minutes. This unprecedented data set and mapping capability creates research opportunities in ionospheric science and space weather monitoring applications.

There has been considerable interest recently in developing methods for interpolating ionospheric measurements on global scales (Juan et al., 1997; Schreiner et al., 1997; Hajj et al., 1994; Howe et al., 1998; Komjathy et al., 1998; Mannucci et al., 1998; Ruffini et al., 1998). We have previously reported a two-dimensional mapping technique for retrieving the global distribution of zenith-looking TEC, assuming the electron density profiles in the vertical direction are fixed (Mannucci et al., 1998). In this study, we discuss a fully three-dimensional mapping approach using three independent vertical layers to describe the electron density distribution. We observe a reduction in systematic effects, and improved consistency between data and the resulting fit. We describe the new global ionosphere mapping (GIM) technique with degrees of freedom in both the vertical and horizontal dimensions. We apply this method to a simulated data set to assess the accuracy improvements compared to a two-dimensional technique. We also present the results of a comparison using actual GPS data. Finally, we discuss how the new approach is best utilized for local and global TEC studies.

2. Global Ionosphere Maps With Three Spatial Dimensions

Three dimensional mapping is a procedure to retrieve the ionospheric electron density as a function of latitude, longitude and height based on measurements of the integral of

electron density along receiver-transmitter lines of sight. It contrasts with a previously reported two dimensional mapping technique (Mannucci et al., 1998), where TEC is retrieved directly as a function of only latitude and longitude.

2.1 Modeling the Observations

The first step in a mathematical description of the three dimensional mapping problem is to express each measurement of TEC T_{rs} as an integral of electron density N_e along the receiver-satellite line of sight:

$$T_{rs} = \int_{\mathbf{R}_{rcv}}^{\mathbf{R}_{trn}} N_e(\theta,\phi,h)ds \tag{1}$$

where the free electron density is expressed as a function of latitude, longitude and height (θ,ϕ,h) and the integral is evaluated along the straight-line path between receiver and transmitter locations $\mathbf{R}_{rcv}$ and $\mathbf{R}_{trn}$ (GPS altitudes are ~20,200 km). We next assume that the density can be written as a linear combination of basis functions. This parametrizes the underlying density distribution because the coefficients in the linear sum are estimated from the data. Let $H_i(\theta,\phi)$ represent the ith basis function for the horizontal dimension, and $V_j(h)$ the jth basis function in the vertical. We write:

$$N_e(\theta,\phi,h) = \sum_{i=1}^{N_H}\sum_{j=1}^{N_V} c_{ij}H_i(\theta,\phi)V_j(h) \tag{2}$$

where the unknown coefficients are c_{ij}. The number of coefficients necessary to specify the density distribution is the product of the number of basis functions in each dimension $N_H N_V$ (in this study we use N_H=330 and N_V =3).

The choice of basis functions determines the spatial structure that can be reproduced. For the horizontal basis functions $H_i(\theta,\phi)$ we have chosen the set used in two-dimensional GIM. Currently these consist of 330 gaussian-shaped bicubic splines that combine to produce smoothly varying TEC contours over a spherical surface, based on algorithms developed by Charles Lawson at JPL (Lawson, 1984). In the vertical dimension, we have chosen basis functions that consist of constant density slabs stacked vertically. We use three slabs with heights as described below. Neither of the basis sets are orthogonal. This is acceptable because in the fitting process correlations between parameters are fully accounted for, and we use square-root inversion methods that are numerically stable (Bierman, 1977). A preliminary set of empirical orthogonal functions (Twomey, 1997) in the vertical dimension has been developed but these results will not be reported here (also see Howe et al., 1998).

Substitution of the basis function expansion of N_e into the equation for the observable T_{rs} leads to the following parametrized model of the observations:

$$T_{rs} = \sum_{i=1}^{N_H} \sum_{j=1}^{N_V} c_{ij} \int_{\mathbf{R}_{rcv}}^{\mathbf{R}_{trn}} H_i(\theta,\phi) V_j(h) ds \tag{3}$$

where the order of summation and integration has been exchanged, and the coefficients c_{ij} have been moved outside the integral since they are independent of geometry. Equation 3 refers to a single measurement, but of course several measurements are combined to estimate the parameters c_{ij}. We cast this equation into familiar matrix form as follows. First, all coefficients are written as a single column vector **C**, by constructing an arbitrary one-to-one mapping $\Pi(i,j)$ between coefficient (i,j) and a new index $k: k = \Pi(i,j)$ with k=1,...,N_m ($N_m = N_H N_V$). Letting **T** be the vector of observations, we can write a variant of equation 3 that applies to several measurements:

$$\mathbf{T} = \mathbf{AC} \tag{4}$$

where the "observation matrix" **A** is composed of integrals over the basis functions. Element (m,n) of **A** is given by:

$$A_{mn} = \int_{\mathbf{R}_{rcv}}^{\mathbf{R}_{trn}} H_i(\theta,\phi) V_j(h) ds \tag{5}$$

where the receiver and transmitter positions apply to measurement m. Basis function combination (i,j) maps to coefficient number n via $n = \Pi(i,j)$.

The TEC mapping procedure consists of solving equation 4 for the coefficients **C** based on the observations **T**. We solve this linear system using a Kalman filter so that the coefficients c_n can be modeled as stochastic time series (Iijima et al., 1999; Gelb, 1989; Bierman, 1977; Jazwinski, 1970).

The steps for solving the three-dimensional problem are essentially the same as for two dimensions (linear parameter estimation), however the different physical meaning of the parameters should be considered. In two dimensions, the coefficients are in units of integrated column density (electrons/m^2) since they are factors of dimensionless basis functions that describe a zenith-looking TEC distribution. In three-dimensional mapping, the coefficients are in units of electron density (electrons/m^3) so that retrieving TEC maps from the solution requires an additional integration step. Retrieving the individual coefficients is an ill-posed problem due to the restricted observing geometry of ground-based measurements (see for example Hajj et al., 1994). The electron density in each layer remains uncertain since each observation samples the *sum* of the vertical basis function

coefficients c_{i1}, c_{i2}, and c_{i3}. In this paper, we will only consider the TEC derived from the multilayer approach, which we expect is improved compared to the two-dimensional model. We will treat recovery of vertical structure in a future paper (see also Howe et al., 1998; Rius et al., 1997).

2.2 Instrumental Bias Estimation

For real GPS systems, instrumental biases cause systematic errors of up to ≅50 TECU if left uncalibrated (Sardon et al., 1994; Sardon and Zarraoa, 1997; Wilson et al., 1995) (1 TEC Unit is a column density of 10^{16} electrons per meter^2). These biases are caused by hardware delay differences between the two GPS frequencies. Since no independent source of such data is available, we estimate the instrumental offsets simultaneously with the ionospheric delay map by augmenting the observation model equation 3 with additional parameters:

$$T_{rs} = \sum_{i}^{N_H} \sum_{j}^{N_V} c_{ij} \int_{\mathbf{R}_{rcv}}^{\mathbf{R}_{trn}} H_i(\theta,\phi) V_j(h) ds + b_r + b_s \tag{6}$$

where b_r and b_s are the instrumental biases for the receiver and satellite, respectively. A single bias term is fitted per day for each receiver and satellite. In contrast, the density coefficients c_n are updated every 15 minutes.

The biases can be retrieved simultaneously with the TEC maps because they are constant offsets with a different time or elevation-angle dependence than the ionosphere delay. The bias component of delay can be separated from the ionospheric component with high precision (<< 1 TECU) and reasonable accuracy ≅1-3 TECU (Mannucci et al., 1998; Iijima et al., 1999).

2.3 Constraining the Retrievals

Retrieval methods that rely primarily on fitting predefined basis functions to data often benefit from regularization procedures that constrain the space of possible solutions. For the two-dimensional single-layer retrievals, simulated vertical TEC measurements from a climatological model are added to the fit periodically at regularly spaced grid locations (see the discussions in Iijima et al., 1999 and Mannucci et al., 1998). The model TEC smoothes the maps spatially, and reduces extrapolation errors in the regions between clusters of receivers where the fit is not well-constrained by data. The simulated measurements produce insignificant change in the retrieved TEC in the vicinity of data since they are assigned a low data weight (large measurement noise) relative to the actual measurements.

For three dimensional retrievals, it is well known that the lack of horizontal raypaths in the inversion problem leads to poor resolution of vertical structure even in areas where the GPS measurements are available (Hajj et al., 1994). We use a model-assisted regularization procedure to constrain the vertical distribution of electron density. We compute the integrated electron content (IEC) within a single layer by integrating the Bent model (Llewellyn and Bent, 1973) density vertically within the height limits of the layer, and thus simulate a measurement value, substituted into T_{rs} of equation 3 (although no actual satellite or receiver need be present). The appropriate elements of the A matrix are also computed by integrating the basis functions (right hand side of equation 3). The IEC estimates are differenced between adjacent layers (Figure 1) and added to the retrieval procedure as measurements of the *differential IEC* between layers. This additional constraint prevents unphysically large electron densities in any particular layer, which may be compensated for by small or negative densities in other layers. As with the two-dimensional regularization, the vertical TEC map still closely follows the data, but certain numerical procedures in the fitting process are more straightforward if the densities are well bounded. Since the retrieval is insensitive to the vertical layer structure, the two differential IEC measurements have a weak influence on the retrieved total TEC.

We are currently using a value of 2 TECU as the "measurement noise" on the simulated IEC constraint, compared to a typical value of 1.3 TECU for the measurement noise of the actual TEC data. The optimal value of the constraint weighting deserves further study.

3. Results

The purpose of this research is to assess the improvement of three versus two spatial dimensions in the ionosphere mapping model. We apply each approach to retrieving TEC maps using both simulated and actual data from a global ground network. Assessing simulation results is straightforward since "ground truth" is available. We have assessed the live data retrieval in two ways: comparisons with independent TOPEX measurements (see Iijima et al. 1999) and goodness-of-fit metrics. In both cases, the emphasis is on comparisons between the two and three-dimensional retrieval of TEC.

3.1 Simulation Study

The simulation study is diagrammed in Figure 2. We started with an observation file containing actual measurements and satellite locations (azimuth and elevation) and substituted simulated measurements derived by integrating the density profiles of the Bent ionosphere model (Llewellyn and Bent, 1973) along the satellite-receiver raypaths. This simulated data file is then processed using both single-shell and multilayer techniques. The predefined electron density form for the shell model is a constant density slab extending from 350 to 600 km. This form was chosen as it is one of the layers in the three-slab retrieval, although it is simplified compared to our operational GIM retrievals. The comparisons here assess the improvement resulting from the surrounding upper and lower layers.

No biases are added to the simulated observations, so the ground truth bias values are zero for all receivers and satellites. The satellite biases were retrieved with high accuracy using both two and three-dimensional techniques. Estimated receiver biases are shown in Figure 3. For the single shell approach, we observe a systematic offset from the correct value of zero. The multilayer approach produces a significantly reduced overall bias (see table inset). Other studies (Juan et al., 1997) also report receiver bias differences when more than one vertical degree of freedom is used in the TEC retrievals. These results suggest that improved spatial modeling can improve GPS measurements of TEC through better estimation of receiver biases.

In both techniques, a few low latitude sites had significant receiver bias error. This deserves further study to identify the specific factors leading to increased error for these sites. Other single-layer studies performed with live data do not show a consistent correlation between latitude and receiver bias error. Comparisons between GIM and independent measurements of vertical TEC show no significant increase in GIM bias at

low latitudes (Ho et al., 1997; Mannucci et al., 1994). Since the independent data were restricted to within a few hundred kilometers of the receivers, a significant receiver bias error would be readily observed. However, the data for several receivers were averaged together, possibly masking the accuracy degradation from one or two sites.

The vertical TEC maps were also compared between the two techniques. The retrievals were compared with the vertically integrated density of the ground truth model over a 5x5 degree grid spanning all longitudes and latitudes from 80S to 80N. For a two-dimensional retrieval, vertical TEC at a particular location is obtained by evaluating the solved-for linear combination of horizontal basis functions $H_i(\theta,\phi)$. For the multilayer approach, we integrated the retrieved density (equation 2) over the entire height range of the slabs (see Figure 2 for slab heights). For each map hour, we computed the TEC retrieval errors averaged over all comparison grid point locations; the statistics are shown in Figure 4. A more accurate overall mean level is obtained with the multilayer model compared to the single shell, consistent with the improved bias estimation as discussed above.

The standard deviations of the retrieval error are similar between the two methods, suggesting that the multilayer approach is not superior in retrieving the spatial variation of global TEC. This result can be understood if we consider two important factors that affect the accuracy of the global mapping procedure: retrieval errors in the vicinity of receivers, and errors incurred mapping TEC between receiver sites. The accuracy of TEC estimates near receivers obviously benefits from improved instrumental bias estimation. However, the additional vertical degrees of freedom apparently do not improve the maps beyond what is obtained locally to the site. In the absence of direct observations, the mapping process relies on the approximation that the vertical TEC is relatively constant at a given local-time (Mannucci et al., 1998). In regions that are not directly sampled by data, errors from this assumption of TEC persistence are common to both fitting techniques.

3.2 Live Data Study

We also performed a comparison of two and three-dimensional retrieval methods using actual data for a single day. Although there is no source of ground truth in this case, we compared the retrievals to independent measurements of vertical TEC available from the TOPEX altimeter (Imel, 1994). Using live data introduces uncertainty into the comparisons because TOPEX measurements themselves are biased. The simulation-based study indicates that three dimensional modeling may produce a relatively small improvement to the global map bias, of the order ≅1-2 TECU. This is within the error tolerance in the TOPEX measurements themselves.

As with the simulations, we compare a two dimensional shell model retrieval (350-600 km slab) with a three dimensional retrieval that is similar except for the additional

vertical degrees of freedom. We processed identical data sets in the two methods, and compared the vertical TEC maps against TOPEX measurements along the 26 ground tracks available on July 20, 1998. The local times of the tracks during equatorial crossing were ~10am and ~10pm. A map of ground track locations is shown in Figure 5 along with locations of the GPS receivers used in the retrievals (only receivers providing nearly complete data sets are shown). The boundaries of the three slabs are 250, 350, 600 and 1200 km.

We computed the mean and standard deviation of the TOPEX-GIM differences for all TOPEX passes on July 20, 1998. Since there is an unknown mean offset associated with the TOPEX measurements, only the standard deviations of the differences for each track are shown in Figure 6. The results are broken down by hemisphere: 0-66 degrees (top panel) and -66-0 degrees (lower panel) (TOPEX passes extend to ±66° latitude). There is no clear advantage to the three dimensional retrieval assuming that TOPEX is ground truth. The spatial variation of the maps is not improved with the additional layers. These results are consistent with the hypothesis that the multilayer technique reduces systematic bias in the retrievals and thereby improves the TEC model near the receivers. Ignoring an overall bias, the retrievals are not improved and may even be worse than the shell model in regions far from receivers.

We have observed significant improvement from the multilayer technique when considering the "post-fit" residuals. These are the difference between the measurement and the slant delay computed by substituting the fitted coefficients into equation 3. Three dimensional modeling produces a significant reduction in the standard deviation of these residuals as shown in Figure 7. These are the daily values for the 11 receiver sites with the largest residuals. As expected, worse agreement is obtained for low latitude sites where the large horizontal TEC gradients from the equatorial anomaly are more difficult to model.

The largest residuals for the shell approach are found at the Cocos islands site (-12.2 latitude, 96.8 East longitude), where the multilayer residuals are significantly lower. Further analysis reveals that the improved modeling primarily affects low elevation angle measurements. This is shown in Figure 8 where the root-mean-square (RMS) post-fit residuals have been binned by elevation angle. This result can be explained considering the different models of slant TEC that are used. In the two-dimensional retrievals, slant observations are the product of vertical TEC and a predetermined obliquity factor that determines the delay variation with elevation angle (Mannucci et al., 1999). At high elevations, the obliquity factor is by definition equal to one, but at lower elevations it can vary between about 2.2 and 3.0, depending on the distribution of electron density in the vicinity of the raypath. However, a fixed factor is applied universally. In the three dimensional model, slant TEC is derived by integrating the estimated density profiles. Since the profiles are optimal fits to the data, there can be a higher degree of consistency between the vertical and slant measurements that are processed simultaneously,

producing a better fit. The advantage of multilayer modeling can be clearly observed for elevation angles below about 50 degrees.

4. Discussion and Conclusions

We have developed a global ionosphere mapping technique that introduces multiple electron density layers into the model of GPS observations. In this study, we found that the three-dimensional approach reduces systematic level errors in the TEC maps, when comparing with a single layer retrieval. Moreover, we observed that the modeling of slant TEC is improved, particularly for low-latitude receivers, where the benefit is observed at elevation angles as high as 50 degrees.

Three-dimensional retrievals may provide important benefits to NASA when tracking spacecraft that orbit out of the ecliptic plane such as Ulysses, which requires long observation periods at low elevation angles. We have found through analysis of post-fit residuals that using multiple independent layers provides a better model of slant TEC measurements as compared to a two-dimensional ionosphere model. Further studies are required to assess whether the improved consistency is correlated with improved accuracy of slant TEC modeling.

Systematic errors in the level of the vertical TEC maps are possibly reduced by three dimensional modeling, desirable when calibration accuracies exceeding ~1-2 TECU are required, particularly in regions near receiver sites. However, after accounting for an overall bias, we do not observe significant improvement in the retrieved global distribution of TEC. Previous accuracy studies reported by Ho et al. (1997) provide a possible explanation for this null result. Ho et al. correlated global map accuracy at a particular location with distance to the nearest GPS receiver. Accuracy is reduced the further away the data sources. This is not surprising since we use a simplifying assumption about TEC behavior in areas that are not under direct observation. The TEC is assumed to persist unchanged at a given local time in the absence of observations. To improve significantly the global performance of these maps, a more sophisticated model of ionosphere dynamics is required.

We emphasize that these results should be regarded as preliminary. Based on our experience with the two dimensional retrieval technique, tuning the parametrization and fitting strategy will further improve accuracy in three dimensions. In particular, we will continue to assess the vertical structure, including number and location of vertical layers, and the form of the vertical basis functions. Adjusting the weighting of the model-assisted constraints is also under consideration. We expect that eventually, the largest benefit from multilayer modeling will come from addition of space-based GPS data obtained in an occultation geometry (Hajj and Romans, 1998; Rius et al., 1998; Ruffini et al., 1998). These data open the possibility of three-dimensional electron density mapping on a global basis with high spatial and temporal resolution.

Acknowledgments

The research described in this paper was carried out by the Jet Propulsion Laboratory, California Institute of Technology, under a contract with the National Aeronautics and Space Administration.

References

Bierman G. J. (1977) Factorization methods for discrete sequential estimation. Academic Press, New York.

Gelb A. (1989) Applied optimal estimation. MIT Press, Cambridge, Massachusetts.

Hajj G. A., Ibanez-Meier R., Kursinski E. R., Romans L. J. (1994) Imaging the ionosphere with the global positioning system. International Journal of Imaging Systems and Technology 5, (2) 174-184.

Hajj, G. A. and Romans, L. J. (1998) Ionospheric electron-density profiles obtained with the global positioning system - results from the GPS/MET experiment. Radio Science 33 (1), 175-190.

Ho, C. M., Wilson, B. D., Mannucci, A. J., Lindqwister, U. J., Yuan, D. N. (1997) A comparative study of ionospheric TEC measurements and models with TOPEX. Radio Science 32 (4), 1499-1512.

Howe B. M., Runciman K., Secan, J. A. (1998) Tomography of the ionosphere - 4-dimensional simulations. Radio Science 33 (1), 109-128.

Iijima, B. A., Harris I. L., Ho C. M., Lindqwister U. J., Mannucci A. J., Pi X. Q., Reyes M. J., Sparks L. J., Wilson B. D. (1999) Automated daily process for global ionospheric total electron content maps and satellite ocean altimeter ionospheric calibration based on global positioning system data. Journal of Atmospheric and Solar-Terrestrial Physics, this issue.

Imel, D. A. (1994) Evaluation of the TOPEX/POSEIDON dual-frequency ionosphere correction. Journal of Geophysical Research O 99 (C12), 24895-24906.

Jazwinski, A. H. (1970) Stochastic processes and filtering theory. Academic Press, New York.

Juan J. M., Rius A., Hernandez-Pajares M., Sanz J. (1997), A 2-layer model of the ionosphere using global positioning system data. Geophysical Research Letters 24 (4), 393-396.

Komjathy A., Langley, R.B., Bilitza D. (1998) Ingesting GPS-derived TEC data into the international reference ionosphere for single frequency radar altimeter ionospheric delay corrections. Advances in Space Research 22 (6), 793-801.

Lawson, C. (1984) A piecewise C2 basis for function representation over the surface of a sphere, JPL internal document.

Mannucci, A. J., Wilson, B. D., Yuan, D. N. (1994) Monitoring ionospheric total electron content using GPS global network and TOPEX/POSEIDON data. Proceedings of the Beacon Satellite Symposium, July 11-15, Aberystwyth, United Kingdom, 338-341.

Mannucci A.J., Wilson B. D., Yuan D. N., Ho C. M., Lindqwister U. J., Runge T. F. (1998) A global mapping technique for GPS-derived ionospheric total electron-content measurements. Radio Science 33 (3), 565-582.

Mannucci A. J., Iijima, B. A., Lindqwister U. J., Pi, X. Q., Sparks, L. J., Wilson B. D. (1999) GPS and ionosphere. In: Ross-Stone, W. (Ed.), URSI Reviews of Radio Science, International Union of Radio Scientists.

Ruffini G. L., Flores A., Rius A. (1998) GPS tomography of the ionospheric electron-content with a correlation functional. IEEE Transactions On Geoscience And Remote Sensing 36 (1), 143-153.

Rius A., Ruffini G., Cucurull L. (1997) Improving the vertical resolution of ionospheric tomography with GPS occultations. Geophysical Research Letters 24 (18), 2291-2294.

Rius, A., Ruffini, G., Romeo A. (1998) Analysis of ionospheric electron-density distribution from GPS/MET occultations. IEEE Transactions On Geoscience And Remote Sensing 36 (2), 383-394.

Ruffini G. L., Cardellach E., Flores A., Cucurull, L., Rius A. (1998) Ionospheric calibration of radar altimeters using GPS tomography. Geophysical Research Letters 25 (20), 3771-3774.

Sardon E., Rius A., Zarraoa N. (1994) Estimation of the transmitter and receiver differential biases and the ionospheric total electron content from global positioning system observations. Radio Science 29, 577-586.

Sardon E. and Zarraoa N. (1997) Estimation of total electron-content using GPS data – how stable are the differential satellite and receiver instrumental biases? Radio Science 32, 1899-1910.

Schreiner, W. S., Markin, R. E., Born, G. H. (1997) Correction of single-frequency altimeter measurements for ionosphere delay. IEEE Transactions on Geoscience and Remote Sensing 35 (2), 271-277.

Twomey, S. (1997) Introduction to the mathematics of inversion in remote sensing and indirect measurements. Dover Publications, New York,

Wilson B. D., Mannucci A. J., Edwards C. D. (1995) Subdaily northern-hemisphere maps using an extensive network of GPS receivers. Radio Science 30 (3), 639-648.

Reports

Llewellyn, S. K. and R. B. Bent (1973) Documentation and description of the Bent ionospheric model, Report AFCRL-TR-73-0657, Air Force Research Laboratory, Hanscom Air Force Base, Massachusetts.

Figure Captions

Figure 1. Representation of what is observed using live data (TEC) versus what is generated using an electron density model: measurements of the differential integrated electron content between adjacent layers.

Figure 2. Method for assessing three-dimensional retrievals against a two-dimensional model run. The obliquity factor for the single slab model is for a constant density slab extending from 350-600 km.

Figure 3. Comparison of retrieved receiver biases for the single and multilayer approaches using simulated data. Ground truth values are all zero. Sites with the largest error values are labeled by latitude.

Figure 4. Statistics on the differences between retrieved TEC and ground truth over a 5°x5° latitude/longitude global grid. Maps were updated once per hour.

Figure 5. Locations of global network receivers (●) and TOPEX ground tracks for July 20, 1998. TOPEX pass numbers are shown.

Figure 6. Standard deviations of the differences between TOPEX and GIM plotted by TOPEX pass number for both retrieval methods. Comparisons are plotted separately for Northern (latitude > 0) and Southern (latitude < 0) regions.

Figure 7. Postfit residuals of slant data by site for single and multilayer methods. Only the sites with the 11 largest residuals are shown.

Figure 8. Postfit residuals for the Coco Islands site binned by elevation angle.

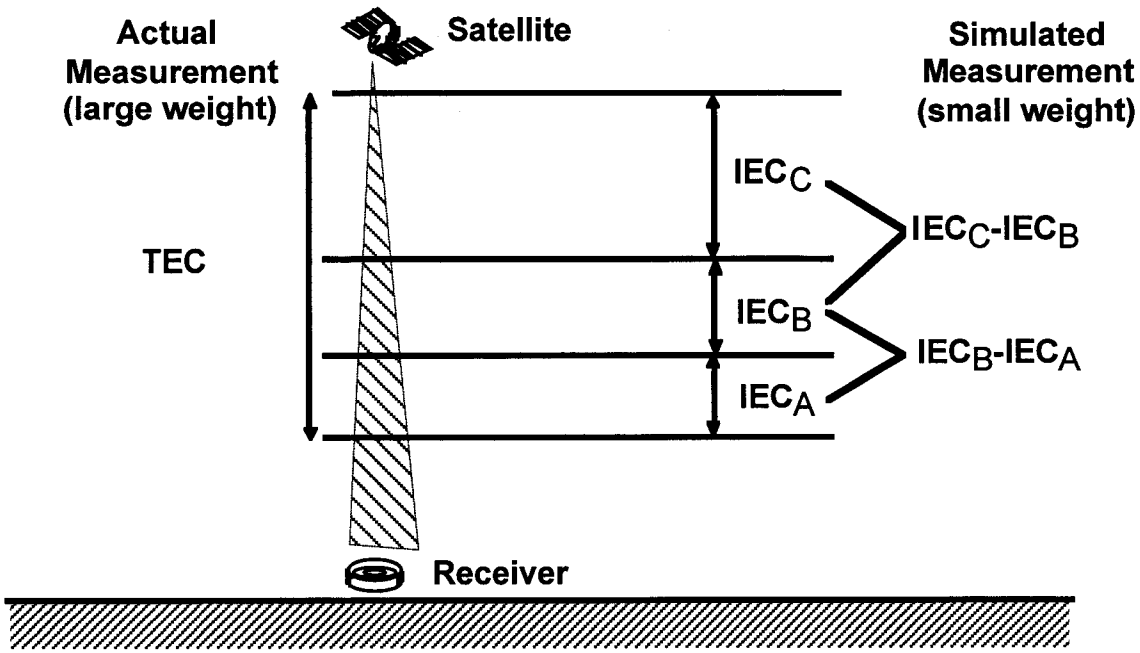
Actual
Measurement
(large weight)
Satellite
Simulated
Measurement
(small weight)
IEC$_C$
IEC$_C$-IEC$_B$
TEC
IEC$_B$
IEC$_B$-IEC$_A$
IEC$_A$
Receiver

Figure 1.

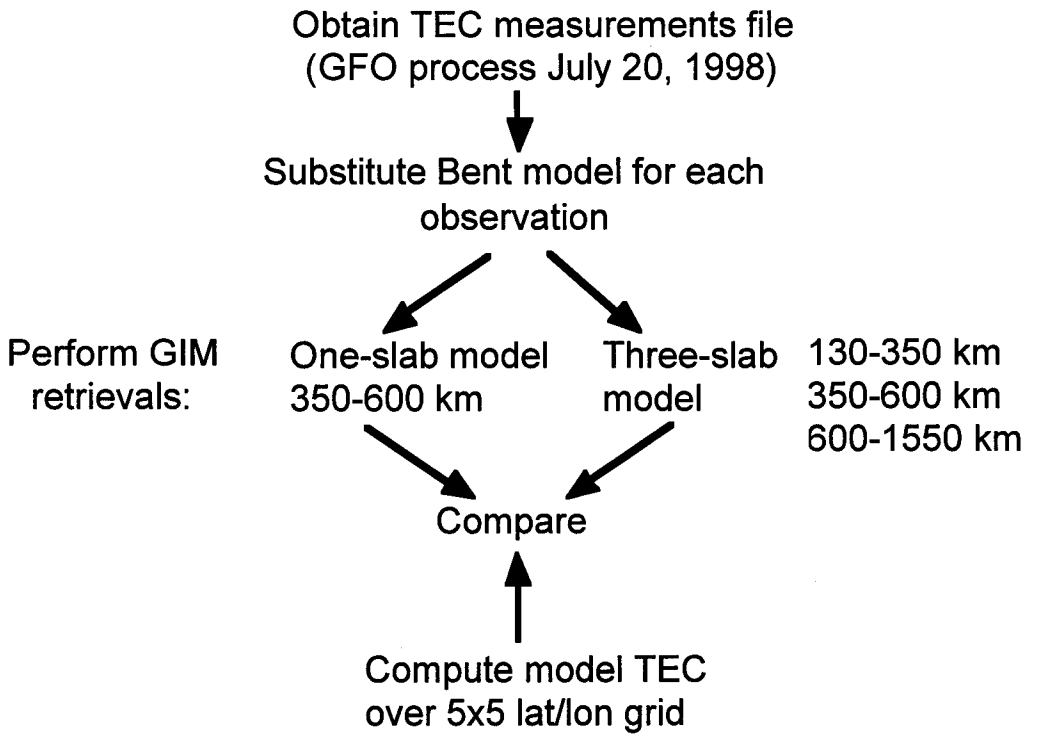
Obtain TEC measurements file
(GFO process July 20, 1998)
Substitute Bent model for each observation
Perform GIM retrievals:
One-slab model 350-600 km
Three-slab model
130-350 km
350-600 km
600-1550 km
Compare
Compute model TEC over 5x5 lat/lon grid

Figure 2.

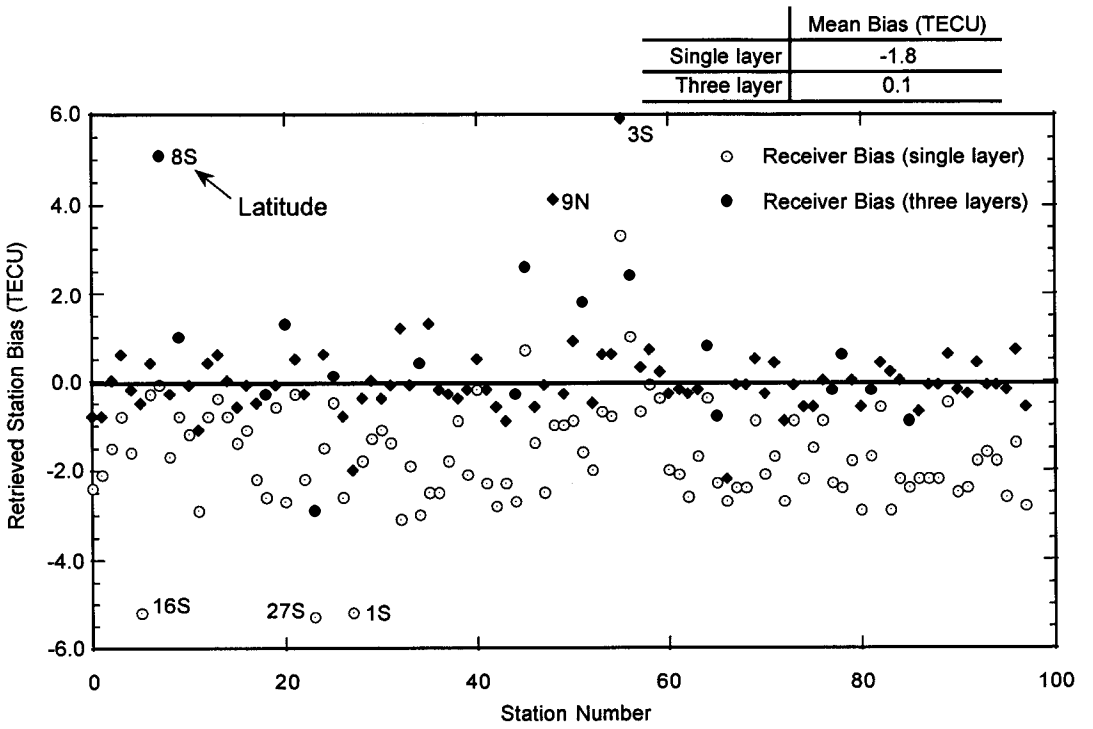
Mean Bias (TECU)
Single layer -1.8
Three layer 0.1
8S
Latitude
3S
9N
16S
27S
1S
Receiver Bias (single layer)
Receiver Bias (three layers)
Retrieved Station Bias (TECU)
Station Number
6.0
4.0
2.0
0.0
-2.0
-4.0
-6.0
0
20
40
60
80
100

Figure 3.

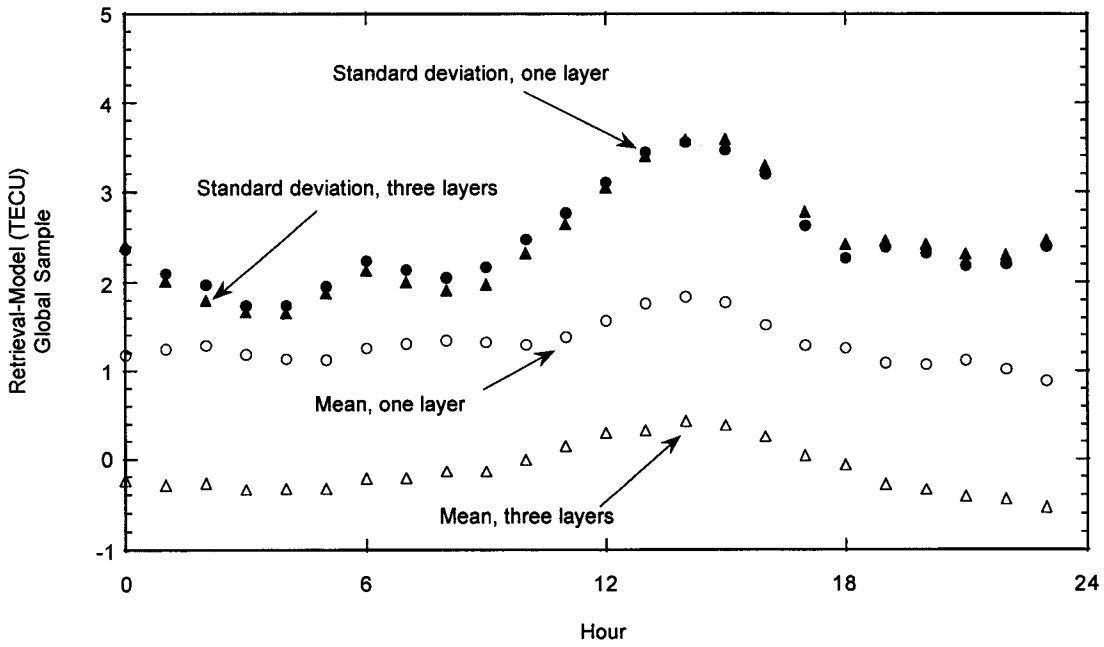

Figure 4.

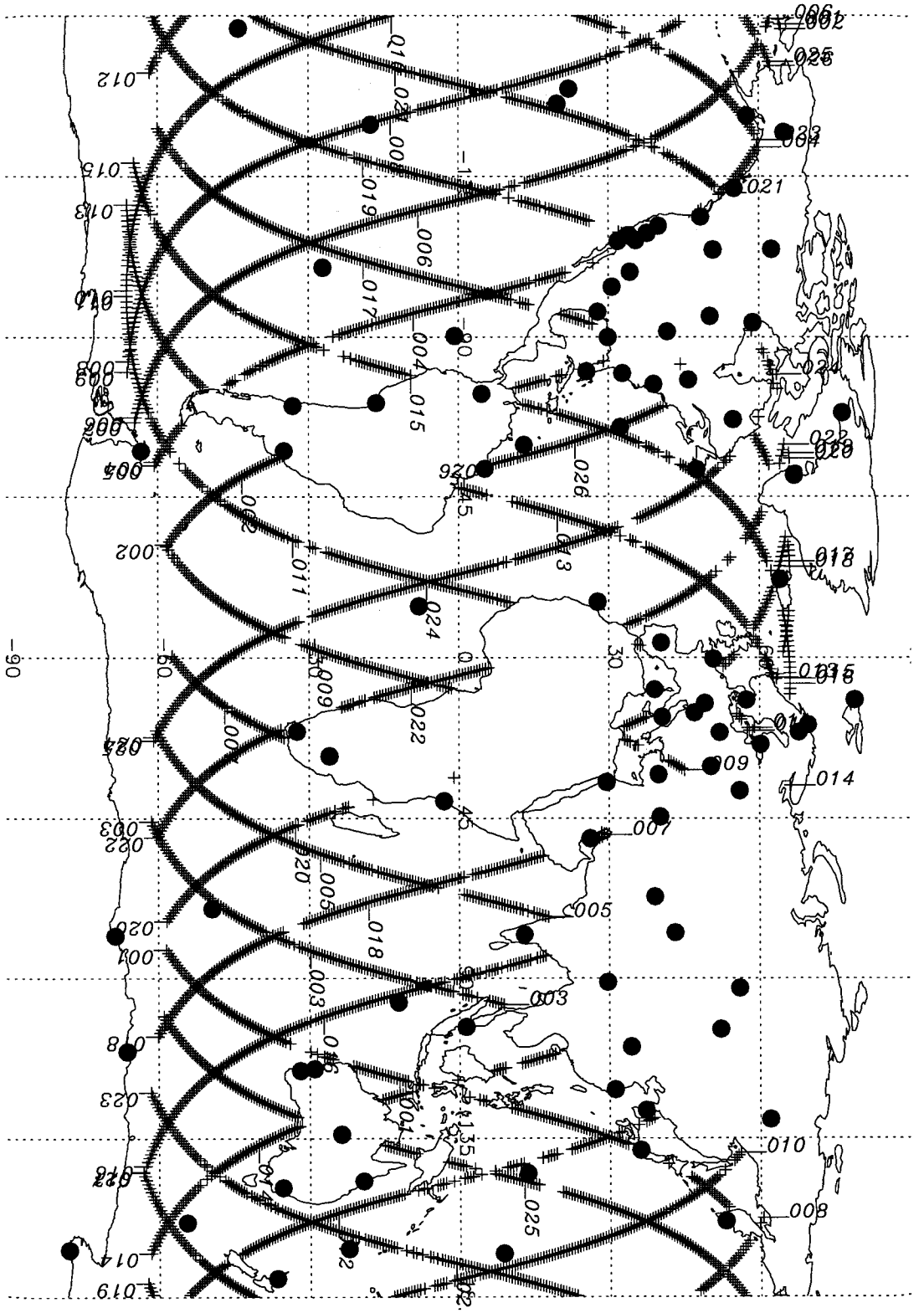

Figure 5.

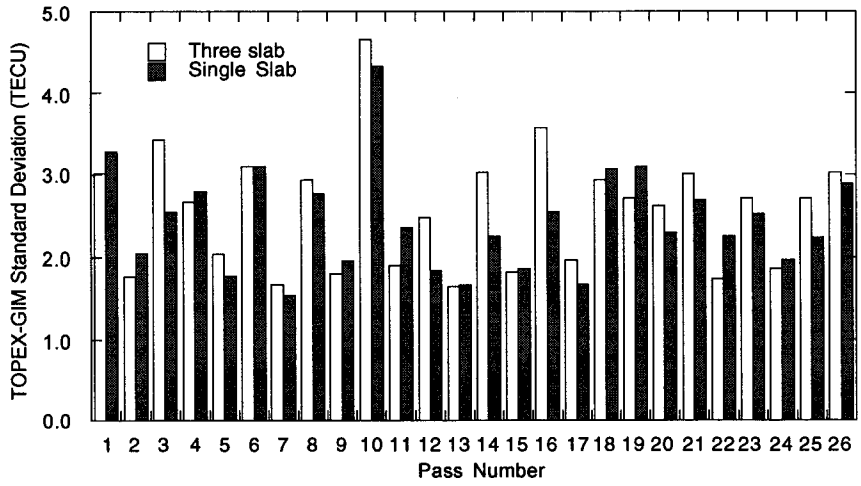
Three slab
Single Slab
TOPEX-GIM Standard Deviation (TECU)
5.0
4.0
3.0
2.0
1.0
0.0
1 2 3 4 5 6 7 8 9 10 11 12 13 14 15 16 17 18 19 20 21 22 23 24 25 26
Pass Number

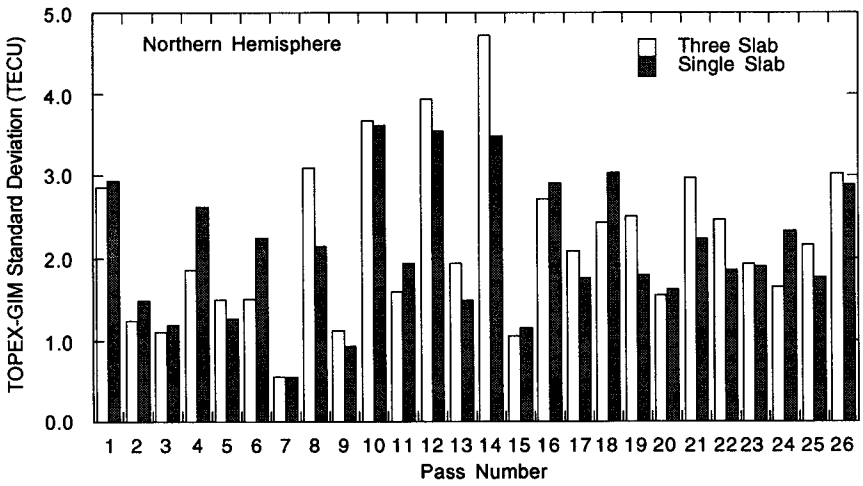
Northern Hemisphere
Three Slab
Single Slab
TOPEX-GIM Standard Deviation (TECU)
5.0
4.0
3.0
2.0
1.0
0.0
1 2 3 4 5 6 7 8 9 10 11 12 13 14 15 16 17 18 19 20 21 22 23 24 25 26
Pass Number

Figure 6.

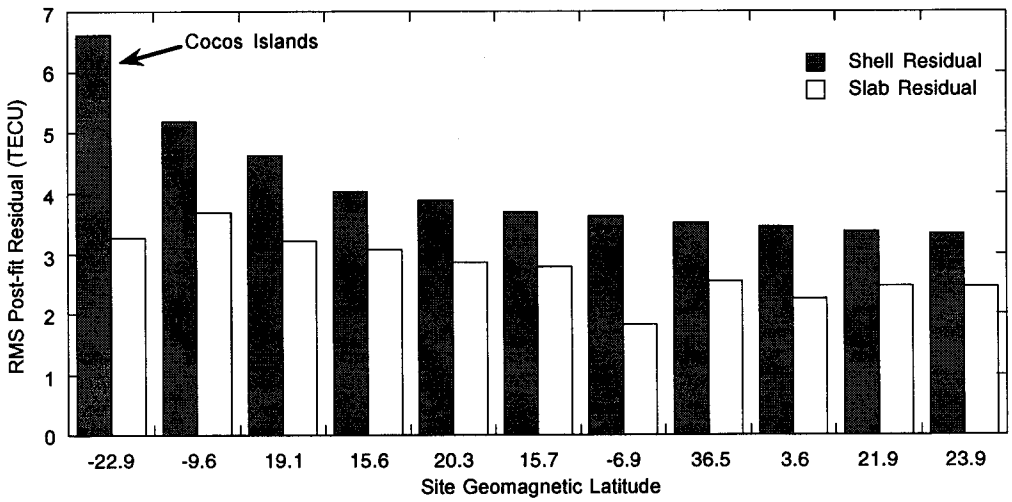

Figure 7.

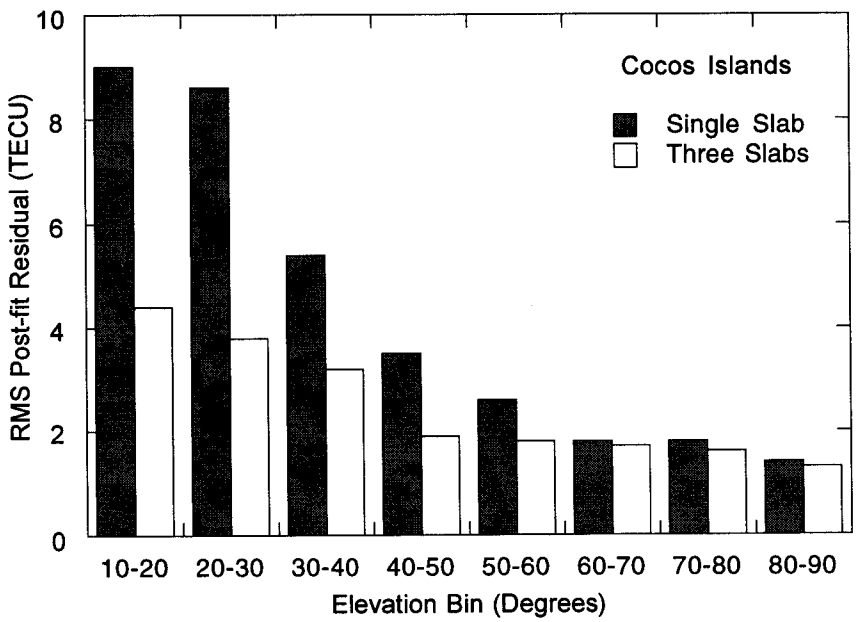

Figure 8.